J Chem Crystallogr (2012) 42:119–129
DOI 10.1007/s10870-011-0212-6

ORIGINAL PAPER

Synthesis and Crystal Structure of a Novel Heterocycle, 2-Oxa-4,7-Diazabicyclo[3.3.1]Non-3-Ene

Sanjay Dutta · Sergey M. Dibrov · Bao T. Ho · Cody J. Higginson · Thomas Hermann

Received: 30 March 2011 / Accepted: 17 November 2011 / Published online: 26 November 2011

Abstract The compound **5**, containing the novel heterocycle 2-oxa-4,7-diazabicyclo[3.3.1]non-3-ene, has been obtained in a synthetic approach toward oxazoles and 1,3-diazepanes of natural product-like complexity from cyclization and rearrangement of δ-lactam cyanamides. When this procedure was applied to a silyl-protected *N*(*3S*,*4S*,*5S*)-4,5-dihydroxy-2-oxopiperidin-3-yl)cyanamide (**2b**) formation of the novel heterobicyclic scaffold **5** was observed along with the expected oxazole (**3b**) and diazepane (**4b**) products. The crystal structures of **5** and diazepane **4b** are described. Compound **5** crystallized from methanol in the monoclinic system, $P2_1$ space group with unit cell parameters $a = 15.3402(9)$, $b = 7.2717(4)$, $c = 22.5803(13)$, $\beta = 106.8620(10)$ and a cell volume of 2410.5(2) A^3.

Keywords 1,3-Diazepane · Oxazole · Cyclization · Bicyclic scaffold

Sanjay Dutta and Sergey M. Dibrov contributed equally to this study.

S. Dutta · S. M. Dibrov · B. T. Ho · C. J. Higginson · T. Hermann (✉)
Department of Chemistry and Biochemistry,
University of California,
9500 Gilman Drive, San Diego,
La Jolla, CA 92093, USA
e-mail: tch@ucsd.edu

Present Address:
S. Dutta · C. J. Higginson
Department of Chemistry,
The Scripps Research Institute,
10550 North Torrey Pines Road,
La Jolla, CA 92037, USA

Introduction

While five- and six-membered rings dominate among ligands that target ribonucleic acid (RNA) folds [1, 2], we have recently explored ligands that contain substituted seven-membered heterocycles of natural product-like complexity [3]. In an unprecedented cyanamide-induced rearrangement of the silyl-protected epoxy-δ-lactam **1a** the 1,3-diazepane **4a** was obtained as well as the oxazole **3a** as a minor product (Scheme 1). We demonstrated that the trans-axial orientation of the alkoxide nucleophile relative to the cyanamide in the intermediate δ-lactam **2a** disfavors the ring closure to the oxazole **3a** and facilitates migration of the silyl group to the 4-position. As we outlined previously [3], the bulky TBDMS group immobilizes the conformation of the lactam ring to favor nucleophilic attack of the carbonyl oxygen at the cyanamide carbon which initiates a series of transformations that eventually lead to the rearranged 1,3-diazepane scaffold **4a**. As the stereoselective progression of the rearrangement depends on the constitution of the epoxy-δ-lactam, we have now investigated the reaction of the diastereomer **1b** with cyanamide. The synthesis of **3a** and **4a** from **1a** is conveniently executed as a one-pot reaction, without isolation of the intermediate **2a**. Reaction conditions in the one-pot reaction are readily adjusted to optimize yield either for the oxazole **3a** of the diazepane **4a** [3]. We assumed that the first step of the reaction sequence, namely the nucleophilic opening of the epoxide by cyanamide, will not be affected by the stereochemistry of the starting material **1b**. In contrast, our earlier studies on the further conversion of the intermediate **2b** suggest that the configuration of the intermediate plays an important role in directing the outcome of the reaction towards the products **3a** and **4a**. Therefore, the δ-lactam diastereomer **2b** was synthesized

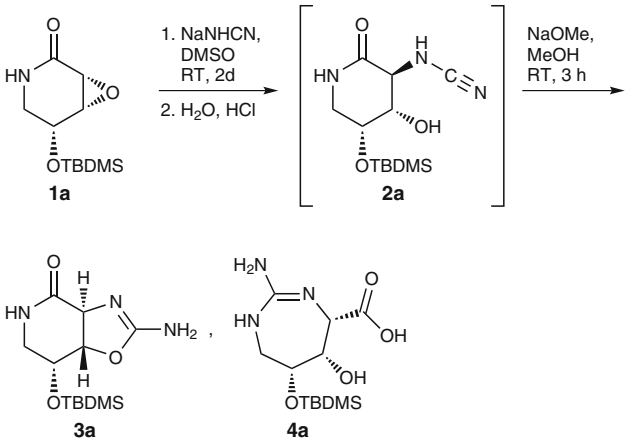

Scheme 1 Formation of the amino-oxazole **3a** and 1,3-diazepane carboxylic acid **4a** from epoxy δ-lactam **1a** which proceeds via the δ-lactam cyanamide **2a** in a one-pot synthesis [3]

from **1b** and isolated as pure compound. Treatment of **2b** with methoxide was performed to initiate the rearrangement reaction (Scheme 2). In addition to the two expected products, the oxazole **3b** and the 1,3-diazepane **4b**, a third major component was isolated and identified as the lactam **5** which contains a novel heterobicyclic 2-oxa-4,7-diazabicyclo[3.3.1]non-3-ene scaffold. The constitution of **5** as well as **4b** was established by X-ray crystal structure analysis which we report here. The diffraction data did not allow unequivocal assignment of the absolute stereochemistry of **5**. However, the proposed mechanistic pathway from optically pure starting material **2b** would lead to the single enantiomer shown here for this compound (Scheme 3).

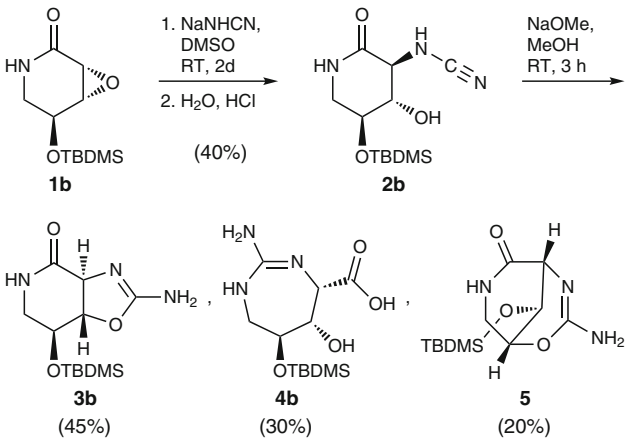

Scheme 2 Conversion of the epoxy δ-lactam diastereomer **1b**, via the δ-lactam cyanamide **2b**, to the expected products **3b** and **4b** as well as the novel 2-oxa-4,7-diazabicyclo[3.3.1]non-3-en-6-one **5**. *Percent numbers* indicate the isolated yield of each purified compound

Experimental

Commercial reagents were used without any further purification. Dry dimethylformamide (DMF) was further purified by passing through a silica gel column. Anhydrous dimethylsulfoxide (DMSO), methanol and ethanol were purchased from AcroSeal. ^{1}H NMR and ^{13}C NMR spectra were recorded on a Jeol ECA 500 MHz NMR, or a 500 MHz Varian NMR system with XSens Cold probe, or a Varian 400 MHz spectrometer. Low resolution mass spectra were obtained on a ThermoFinnigan LCQDECA-MS spectrometer.

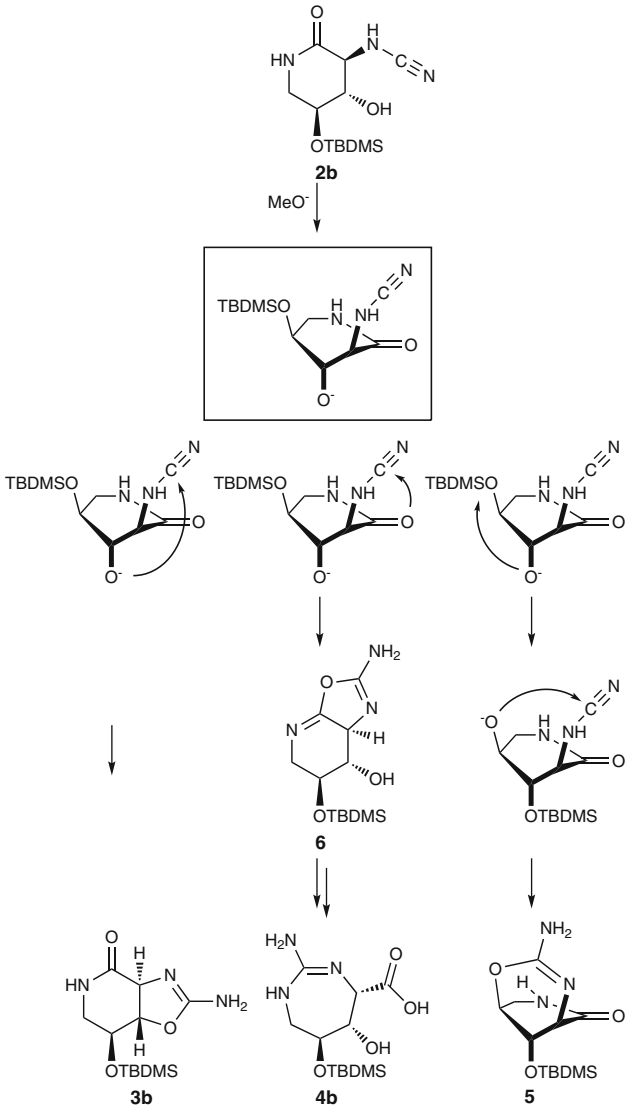

Scheme 3 The proposed mechanism that leads from the δ-lactam cyanamide **2b** to the products **3b**, **4b** and **5**. The conversion of **6** to **4b** has been described previously [3]

N-((3S,4S,5S)-5-((*tert*-Butyldimethylsilyl)Oxy)-4-Hydroxy-2-Oxopiperidin-3-yl)Cyanamide (**2b**)

In a 250 mL oven dried flask purged with argon 6 mL of anhydrous DMSO were added to sodium cyanamide (269 mg, 4.2 mmol, 1.5 equivalents) and the mixture was sonicated for 5 min to expedite dissolution of the salt. To this solution under argon was added dropwise via a syringe 12.8 mL of a solution of **1b** [3] (682 mg, 2.8 mmol) in anhydrous DMSO while constantly stirring. The reaction was stirred further for 48 h at room temperature after which 4.6 mL of 1 N HCl were added while stirring on ice to pH 6.5. The aqueous layer was extracted with ethyl acetate (5 × 35 mL) and the organic layers were dried by evaporating the solvent. Column chromatography of the organic layers on silica gel gave **2b** in 40% isolated yield. **2b**: ^{1}H NMR (500 MHz, CD_3OD) δ 3.84 (m, 1H), 3.80 (q, $J = 5$ Hz, $J' = 15$ Hz, 1H), 3.52 (d, $J = 10$ Hz, 1H), 3.45 (dd, $J = 5$ Hz, $J' = 15$ Hz, 1H), 3.13 (q, $J = 5$ Hz, $J' = 15$ Hz 1H), 0.95 (s, 9H), 0.20 (d, 6H); ^{13}C NMR (500 MHz, CD_3OD) δ 170.8, 117.6, 76.2, 69.9, 62.4, 45.2, 26.5, 19.0, −3.9, −4.4; HRMS (ESI-FT Orbit-Trap-MS) exact mass calculated for $C_{12}H_{23}N_3O_3Si$ 285.1581, found 286.1583 $(M + H)^+$; Delta (ppm) 0.7.

(3aS,7S,7aS)-2-Amino-7-((*tert*-Butyldimethylsilyl) Oxy)-5,6,7,7a-Tetrahydrooxazolo[4,5-c]Pyridin-4(3aH)-One (**3b**), (4S,5S,6S)-2-Amino-6-((*tert*-Butyl dimethylsilyl)Oxy)-5-Hydroxy-4,5,6,7-Tetrahydro-1H-1,3-Diazepine-4-Carboxylic Acid (**4b**), (1R,5R,9S)-3-Amino-9-((*tert*-Butyldimethylsilyl)Oxy)-2-Oxa-4,7-Diazabicyclo[3.3.1]Non-3-En-6-One (**5**)

Compound **2b** (177 mg, 0.62 mmol) was dissolved in 7.4 mL of anhydrous methanol in a dry flask purged with argon. Sodium methoxide (1.8 equivalents, 1.1 mmol, 337 µL of 25% w/w in anhydrous methanol) was added dropwise and stirred at room temperature for 2 h. Then the reaction was quenched with 0.1 N HCl on ice to pH 6.5. The solvent was evaporated and the residue dried under high vacuum. Purification by flash chromatography with hexane, ethyl acetate, methanol and ethanol yielded the products **3b**, **4b** and **5** in isolated yield of, respectively, 45, 30, and 20%. **3b**: ^{1}H NMR (500 MHz, CD_3OD) δ 4.68 (q,

Table 1 Crystal data and structure refinement for compound **4b**

Empirical formula	C12 H25 N3 O4 Si	
Formula weight	303.44	
Temperature	173(2) K	
Wavelength	1.54178 Å	
Crystal system	Monoclinic	
Space group	P2(1)	
Unit cell dimensions	$a = 14.1425(5)$ Å	$\alpha = 90°$
	$b = 6.4236(2)$ Å	$\beta = 101.339(3)°$
	$c = 35.2663(13)$ Å	$\gamma = 90°$
Volume	3141.26(19) Å^3	
Z	8	
Density (calculated)	1.283 Mg/m^3	
Absorption coefficient	1.477 mm^{-1}	
$F(000)$	1,312	
Crystal size	0.10 × 0.10 × 0.05 mm^3	
Theta range for data collection	2.56 to 64.95°	
Index ranges	$(-15 \le h \le 16)$, $(-6 \le k \le 7)$, $(-41 \le l \le 37)$	
Reflections collected	16,818	
Independent reflections	8382 $[R_{(int)} = 0.0563]$	
Completeness to theta = 64.95°	95.3%	
Absorption correction	Semi-empirical from equivalents	
Max. and min. transmission	0.9298 and 0.8663	
Refinement method	Full-matrix least-squares on F^2	
Data/restraints/parameters	8382/1/745	
Goodness-of-fit on F^2	1.049	
Final R indices $[I > 2\sigma > (I)]$	$R_1 = 0.0616$, $wR_2 = 0.1391$	
R indices (all data)	$R_1 = 0.0821$, $wR_2 = 0.1495$	
Largest diff. peak and hole	0.458 and −0.422 eÅ^{-3}	

Table 2 Crystal data and structure refinement for compound **5**

Empirical formula	C12 H23 N3 O3 Si	
Formula weight	285.42	
Temperature	173(2) K	
Wavelength	0.71073 Å	
Crystal system	Monoclinic	
Space group	P2(1)	
Unit cell dimensions	$a = 15.3402(9)$ Å	$\alpha = 90°$
	b = 7.2717(4) Å	$\beta = 106.8620(10)°$
	$c = 22.5803(13)$ Å	$\gamma = 90°$
Volume	2410.5(2) $Å^3$	
Z	6	
Density (calculated)	1.180 Mg/m^3	
Absorption coefficient	0.154 mm^{-1}	
$F(000)$	924	
Crystal size	0.50 × 0.20 × 0.20 mm^3	
Theta range for data collection	0.94 to 25.37°	
Index ranges	$(-16 \le h \le 18)$, $(-8 \le k \le 8)$, $(-27 \le l \le 27)$	
Reflections collected	17,168	
Independent reflections	8,365 [$R_{(int)} = 0.0343$]	
Completeness to theta = 25.37°	99.9%	
Absorption correction	Semi-empirical from equivalents	
Max. and min. transmission	0.9699 and 0.9270	
Refinement method	Full-matrix least-squares on F^2	
Data/restraints/parameters	8365/1/598	
Goodness-of-fit on F^2	1.050	
Final R indices [$I > 2\sigma > (I)$]	$R_1 = 0.0660$, $wR_2 = 0.1638$	
R indices (all data)	$R_1 = 0.0863$, $wR_2 = 0.1845$	
Largest diff. peak and hole	1.029 and −0.451 $eÅ^{-3}$	

$J = 5$ Hz, $J' = 10$ Hz, 1H), 4.37 (d, $J' = 10$ Hz, 1H), 3.98 (m, 1H), 3.20 (dd, $J' = 15$ Hz, 1H), 3.10 (dd, $J = 5$ Hz, $J' = 15$ Hz 1H), 0.79 (s, 9H), 0.04 (d, 6H); ^{13}C NMR (500 MHz, CD_3OD) δ 171.9, 164.6, 83.3, 68.5, 64.1, 43.8, 26.3, 18.9, −4.6; HRMS (ESI-FT Orbit-Trap-MS) exact mass calculated for $C_{12}H_{23}N_3O_3Si$ 285.1581, found 286.1582 $(M + H)^+$; Delta (ppm) 0.3. **4b**: ^1H NMR (500 MHz, DMSO-d6) δ 4.07 (d, 1H); 3.79 (s, 1H); 3.68 (t,1H), 3.26 (d, IH), 3.07 (m, 1H), 0.85 (s, 9H), 0.08 (d, 6H); ^{13}C NMR (500 MHz, DMSO-d6) δ 171.6, 160.1, 70.9, 69.7, 56.5, 43.4, 25.8, 17.8, −4.8; structure confirmed by X-ray crystallography. **5**: ^1H NMR (500 MHz, CD_3OD) δ 4.57 (m, 1H), 4.29 (t, $J = 5$ Hz, 1H), 3.69 (dd, $J = 5$ Hz, $J' = 15$ Hz, 1H), 3.58 (m, 1H), 3.49 (d, $J = 15$ Hz, 1H), 0.90 (s, 9H), 0.15 (s, 6H); ^{13}C NMR (500 MHz, CD_3OD) δ 173.2, 156.9, 71.41, 65.1, 58.1, 45.1, 26.2, 18.9, −4.6; structure confirmed by X-ray crystallography.

X-Ray Crystallography

X-ray diffraction data of the title compound were collected on a Bruker Kappa diffractometer equipped with an APEX CCD II area detector using graphite-monochromated Cu Ka radiation ($\lambda = 1.54178$ Å) for compound **4b** and Mo Ka radiation ($\lambda = 0.71073$ Å) for compound **5**. Colorless plates (0.05 × 0.10 × 0.10 mm and 0.20 × 0.20 × 0.50 mm, respectively) were mounted on a cryoloop with paratone oil. Data were collected in a nitrogen gas stream at 173(2) K using phi and omega scans. The data were integrated using the Bruker SAINT [4] software and scaled using the SADABS [5] program. Solution by direct methods (SHELXS) [6] produced complete phasing models consistent with the proposed structures which were refined by least square methods on F^2 using the SHELXL-97 [6] program package. The refinement was continued until the maximum shift/e.s.d. was 0.000. The final difference map was featureless with maximum and minimum electron densities at, respectively, 0.438 and −0.413 $eÅ^{-3}$ for **4b** and 1.029 and −0.451 $eÅ^{-3}$ for **5**. The crystal data, intensity collection conditions and refinement parameters are presented in Tables 1 and 2. Atomic coordinates and equivalent isotropic displacement parameters are shown in Tables 3 and 4. All non-hydrogen atoms were refined anisotropically by full-matrix least-squares. Selected bond

Table 3 Atomic coordinates ($\times 10^4$) and equivalent isotropic displacement parameters ($Å^2 \times 10^3$) for compound **4b**. U(eq) is defined as one-third of the trace of the orthogonalized U^{ij} tensor

	x	*y*	*z*	U(eq)
Si(1A)	6262(1)	2334(2)	3281(1)	20(1)
Si(1)	8811(1)	2815(2)	6639(1)	19(1)
O(2)	6689(2)	−4083(6)	5347(1)	17(1)
O(1A)	8000(2)	−4601(6)	4740(1)	18(1)
O(2A)	8408(2)	−4132(6)	4161(1)	18(1)
O(3)	7290(2)	1814(6)	5259(1)	18(1)
O(4)	8727(2)	1450(6)	6236(1)	20(1)
O(3A)	8230(2)	603(6)	4593(1)	18(1)
N(2A)	4938(3)	−1898(8)	4678(1)	25(1)
O(4A)	6443(2)	1033(6)	3695(1)	20(1)
N(1A)	6505(3)	−2024(7)	4577(1)	16(1)
N(1)	8314(3)	−1957(7)	5374(1)	13(1)
C(1A)	7924(3)	−3775(9)	4414(1)	14(1)
C(1)	6735(4)	−2465(9)	5556(2)	19(1)
N(3)	9725(3)	−285(7)	5665(1)	17(1)
C(2A)	7128(3)	−2083(9)	4290(1)	16(1)
C(6A)	5653(4)	−1059(9)	4526(1)	18(1)
N(2)	9782(3)	−3211(8)	5290(1)	20(1)
C(2)	7709(3)	−1251(9)	5638(2)	16(1)
C(5A)	6230(4)	2272(9)	4318(2)	20(1)
O(1)	6106(3)	−1781(8)	5711(1)	38(1)
C(4)	8502(3)	2168(9)	5850(1)	18(1)
C(3)	7570(3)	1077(9)	5647(1)	16(1)
C(5)	9337(3)	1804(9)	5648(2)	18(1)
C(9A)	5046(3)	3693(10)	3188(2)	23(1)
C(6)	9271(3)	−1787(8)	5444(1)	14(1)
C(4A)	6937(3)	1689(9)	4068(1)	16(1)
C(3A)	7626(3)	−40(9)	4240(1)	17(1)
C(7)	7791(4)	4681(11)	6587(2)	30(1)
C(12A)	4812(4)	4404(11)	2763(2)	32(2)
C(9)	10011(4)	4259(9)	6748(2)	23(1)
C(11)	10828(4)	2684(12)	6731(2)	38(2)
C(10A)	5033(4)	5607(11)	3445(2)	31(1)
C(8)	8713(5)	829(11)	7012(2)	35(2)
C(8A)	7235(4)	4269(11)	3272(2)	29(1)
C(10)	10036(4)	5988(11)	6464(2)	34(2)
C(12)	10168(4)	5142(11)	7160(2)	35(2)
C(7A)	6273(4)	302(11)	2909(2)	31(1)
C(11A)	4264(4)	2178(11)	3257(2)	34(2)
Si(1B)	3253(1)	400(3)	1720(1)	22(1)
Si(1C)	1724(1)	964(3)	−1681(1)	23(1)
O(2C)	3366(2)	−5762(7)	−317(1)	22(1)
O(4C)	1654(3)	−232(7)	−1274(1)	24(1)
O(1B)	1857(3)	−6198(7)	229(1)	26(1)
O(3B)	1717(3)	−942(7)	347(1)	24(1)
O(3C)	2838(3)	−2(7)	−261(1)	30(1)
N(1C)	1722(3)	−3580(8)	−406(1)	19(1)
N(1B)	3378(3)	−3642(8)	403(1)	18(1)
N(3B)	4410(3)	−1035(8)	699(1)	21(1)
O(2B)	1477(3)	−5796(7)	814(1)	28(1)
C(3B)	2212(4)	−1660(10)	713(2)	24(1)
N(3C)	432(3)	−1564(8)	−725(1)	27(1)
N(2B)	4937(3)	−3421(8)	307(1)	26(1)
C(2C)	2376(4)	−3037(10)	−661(2)	22(1)
C(4B)	2897(4)	−15(10)	934(1)	22(1)
C(1C)	3295(4)	−4415(11)	−576(2)	26(1)
O(1C)	3866(3)	−4028(10)	−790(1)	56(2)
C(4C)	1814(4)	517(10)	−892(2)	26(1)
C(2B)	2715(3)	−3691(9)	678(2)	19(1)
N(2C)	177(3)	−4273(9)	−332(1)	30(1)
C(1B)	1952(3)	−5394(10)	556(2)	22(1)
C(3C)	2644(4)	−715(10)	−649(2)	23(1)
C(6B)	4232(3)	−2685(9)	474(1)	18(1)
C(8B)	3553(4)	3240(10)	1679(2)	28(1)
C(9B)	2045(4)	138(11)	1869(2)	28(1)
C(5B)	3697(4)	607(9)	730(2)	23(1)
C(12B)	1243(4)	1188(12)	1568(2)	35(2)
C(7B)	4217(4)	−945(11)	2070(2)	32(2)
C(5C)	879(4)	463(10)	−730(2)	29(1)
C(6C)	776(4)	−3108(10)	−487(2)	22(1)
C(9C)	2961(4)	688(11)	−1803(2)	32(1)
C(11C)	3738(5)	1723(15)	−1489(2)	50(2)
C(7C)	1412(5)	3805(10)	−1641(2)	33(2)
C(11B)	2078(5)	1191(14)	2260(2)	48(2)
C(10B)	1790(5)	−2168(12)	1899(2)	45(2)
C(10C)	2968(5)	1813(14)	−2180(2)	42(2)
C(8C)	795(4)	−361(11)	−2053(2)	32(2)
C(12C)	3222(5)	−1588(13)	−1832(2)	52(2)
O(4B)	3261(3)	−813(7)	1309(1)	25(1)
N(3A)	5489(3)	721(8)	4341(1)	18(1)

lengths and bond angles are given in Tables 5, 6, 7, and 8. All H atoms were located geometrically, with C–H = 0.95 − 1.0, N–H = 0.88 and O–H = 0.84 Å and treated using a riding model, with isotropic U set to 1.2 or 1.5 times the isotropic equivalent of that of the attached parent atom. For the methyl group, the C–C–H angles and C–H distances were fixed, but the CH_3 group was allowed to rotate about the C–CH_3 bond.

Results and Discussion

Formation of the expected products **3b** and **4b** follows a mechanism that has been established previously for the

Table 4 Atomic coordinates ($\times 10^4$) and equivalent isotropic displacement parameters ($Å^2$ x 10^3) for compound **5**. U(eq) is defined as one-third of the trace of the orthogonalized U^{ij} tensor

	x	*y*	*z*	U(eq)
Si(1)	3431(1)	1971(2)	4157(1)	46(1)
O(1)	258(2)	1893(4)	4272(1)	32(1)
C(6)	1737(3)	2703(6)	4206(2)	30(1)
O(3)	2350(2)	2597(4)	3839(1)	32(1)
O(2)	1289(2)	7327(4)	3646(1)	36(1)
N(3)	563(2)	4697(5)	3245(1)	28(1)
C(3)	1115(3)	5670(6)	3699(2)	28(1)
C(5)	841(3)	1802(6)	3865(2)	30(1)
N(2)	864(2)	4772(5)	4672(2)	31(1)
N(1)	−315(2)	3354(5)	4936(2)	39(1)
C(4)	395(3)	2742(6)	3250(2)	29(1)
C(2)	1518(3)	4689(6)	4316(2)	29(1)
C(1)	313(3)	3413(5)	4628(2)	33(1)
Si(2)	2452(2)	7961(3)	857(1)	45(1)
O(101)	669(2)	12330(4)	1726(1)	39(1)
N(102)	−524(2)	10223(5)	1289(2)	32(1)
O(102)	−108(2)	6676(4)	2075(1)	35(1)
N(103)	1027(2)	8712(5)	2421(2)	31(1)
O(103)	1658(2)	8213(5)	1235(1)	45(1)
C(102)	150(3)	8791(6)	1328(2)	33(1)
C(103)	373(3)	7937(6)	1971(2)	29(1)
C(101)	−225(3)	11808(6)	1505(2)	34(1)
N(101)	−774(3)	13200(5)	1545(2)	47(1)
C(106)	1000(3)	9590(7)	1202(2)	38(1)
C(105)	1367(3)	10994(6)	1717(2)	34(1)
O(201)	5921(2)	6828(4)	646(1)	33(1)
Si(4)	6742(2)	6850(5)	2855(1)	67(1)
O(202)	7285(2)	12233(4)	1351(1)	39(1)
C(202)	6189(3)	9910(6)	1401(2)	35(1)
N(203)	7625(2)	9304(5)	1182(2)	38(1)
N(202)	5505(2)	9893(5)	798(2)	32(1)
N(201)	4821(3)	8242(5)	−76(2)	50(1)
C(201)	5435(3)	8421(6)	481(2)	34(1)
C(203)	7095(3)	10586(6)	1323(2)	32(1)
O(203)	6957(3)	8037(5)	2265(2)	60(1)
C(204)	7519(3)	7306(6)	1216(2)	38(1)
C(205)	6585(3)	6751(6)	1253(2)	34(1)
C(9)	4112(3)	2879(10)	3670(2)	61(2)
C(206)	6278(3)	8026(6)	1691(2)	39(1)
C(104)	1695(3)	10017(6)	2333(2)	34(1)
C(10)	5122(4)	2504(13)	3964(3)	87(2)
C(109)	2789(5)	5595(11)	929(3)	45(2)
C(12)	4003(7)	5010(15)	3625(6)	162(5)
C(11)	3827(5)	2000(20)	3031(3)	167(7)
C(107)	2034(5)	8906(10)	68(3)	83(2)
C(7)	3864(4)	2962(19)	4936(3)	141(5)
C(8)	3460(5)	−525(12)	4212(7)	183(7)

Table 4 continued

	x	*y*	*z*	U(eq)
C(208)	6452(10)	4319(18)	2688(7)	74(4)
C(207)	5748(8)	7869(18)	3065(5)	72(3)
C(209)	7809(7)	7370(30)	3481(4)	111(6)
C(212)	7898(13)	9350(30)	3630(7)	144(8)
C(211)	8584(9)	6470(50)	3263(5)	280(20)
C(210)	7860(12)	6260(30)	4058(6)	140(8)
Si(3)	1846(4)	7385(6)	645(2)	41(2)
Si(5)	7200(4)	7894(9)	3038(2)	50(2)
C(118)	869(13)	5860(50)	301(9)	129(14)
C(221)	8110(20)	4400(40)	3030(20)	129(13)
C(219)	7304(10)	5410(30)	3246(8)	56(5)
C(217)	6160(20)	8880(40)	3149(14)	96(9)
C(218)	8380(30)	8960(40)	3414(11)	107(14)
C(108)	3485(6)	9209(15)	1277(5)	125(4)
C(111)	3426(6)	5053(12)	576(4)	104(3)
C(112)	1869(7)	4307(13)	559(4)	111(3)
C(110)	2999(6)	4879(11)	1575(3)	96(2)
C(222)	7353(13)	5150(30)	3941(8)	58(6)
C(220)	6500(60)	4780(80)	2750(20)	320(60)

Table 5 Bond lengths [Å] for compound **4b**

Si(1)–O(4)	1.655(4)
Si(1)–C(8)	1.856(6)
Si(1)–C(7)	1.857(6)
Si(1)–C(9)	1.905(6)
O(2)–C(1)	1.268(7)
O(3)–C(3)	1.426(6)
O(3)–H(3)	0.8400
O(4)–C(4)	1.411(6)
N(1)–C(6)	1.332(6)
N(1)–C(2)	1.456(6)
N(1)–H(1)	0.8800
C(1)–O(1)	1.214(7)
C(1)–C(2)	1.560(7)
N(3)–C(6)	1.324(7)
N(3)–C(5)	1.446(8)
N(2)–C(6)	1.345(7)
N(2)–H(2A)	0.8800
N(2)–H(2D)	0.8800
C(2)–C(3)	1.510(8)
C(4)–C(5)	1.515(6)
C(4)–C(3)	1.540(7)
C(9)–C(10)	1.501(9)
C(9)–C(12)	1.533(8)
C(9)–C(11)	1.546(8)

Table 6 Bond lengths [Å] for compound **5**

Si(1)–O(3)	1.668(3)
Si(1)–C(8)	1.819(8)
Si(1)–C(7)	1.837(8)
Si(1)–C(9)	1.845(5)
O(1)–C(1)	1.355(5)
O(1)–C(5)	1.457(4)
C(6)–O(3)	1.425(5)
C(6)–C(5)	1.515(6)
C(6)–C(2)	1.519(6)
O(2)–C(3)	1.248(5)
N(3)–C(3)	1.328(5)
N(3)–C(4)	1.445(5)
N(3)–H(3)	0.8800
C(3)–C(2)	1.527(5)
C(5)–C(4)	1.522(6)
N(2)–C(1)	1.285(5)
N(2)–C(2)	1.459(5)
N(1)–C(1)	1.343(5)
N(1)–H(1A)	0.8800
N(1)–H(1B)	0.8800
C(9)–C(11)	1.520(9)
C(9)–C(10)	1.523(8)
C(9)–C(12)	1.559(13)

Table 7 Selected bond angles [°] for compound **4b**

O(4)–Si(1)–C(8)	103.9(3)
O(4)–Si(1)–C(7)	109.5(2)
C(8)–Si(1)–C(7)	110.4(3)
O(4)–Si(1)–C(9)	110.0(2)
C(8)–Si(1)–C(9)	112.3(3)
C(7)–Si(1)–C(9)	110.5(3)
C(3)–O(3)–H(3)	109.5
C(4)–O(4)–Si(1)	128.3(4)
C(6)–N(1)–C(2)	123.9(4)
C(6)–N(1)–H(1)	118.0
C(2)–N(1)–H(1)	118.0
O(1)–C(1)–O(2)	126.9(5)
O(1)–C(1)–C(2)	115.7(5)
O(2)–C(1)–C(2)	117.3(4)
C(6)–N(3)–C(5)	121.0(4)
C(6)–N(3)–H(3A)	119.5
C(5)–N(3)–H(3A)	119.5
C(6)–N(2)–H(2A)	120.0
C(6)–N(2)–H(2D)	120.0
N(1)–C(2)–C(3)	114.7(4)
N(1)–C(2)–C(1)	109.6(4)
C(3)–C(2)–C(1)	112.6(4)
O(4)–C(4)–C(5)	110.8(4)
O(4)–C(4)–C(3)	108.1(4)
C(5)–C(4)–C(3)	112.7(4)
O(3)–C(3)–C(2)	108.8(4)
O(3)–C(3)–C(4)	110.2(4)
C(2)–C(3)–C(4)	110.9(4)
N(3)–C(5)–C(4)	116.6(5)
N(3)–C(6)–N(1)	121.8(5)
N(3)–C(6)–N(2)	119.7(4)
N(1)–C(6)–N(2)	118.4(5)
C(10)–C(9)–C(12)	109.9(5)
C(10)–C(9)–C(11)	110.0(5)
C(12)–C(9)–C(11)	108.0(5)
C(10)–C(9)–Si(1)	111.2(4)
C(12)–C(9)–Si(1)	109.2(4)
C(11)–C(9)–Si(1)	108.4(4)

Table 8 Selected bond angles [°] for compound **5**

O(3)–Si(1)–C(8)	107.6(3)
O(3)–Si(1)–C(7)	110.0(3)
C(8)–Si(1)–C(7)	109.3(6)
O(3)–Si(1)–C(9)	108.1(2)
C(8)–Si(1)–C(9)	113.0(5)
C(7)–Si(1)–C(9)	108.7(3)
C(1)–O(1)–C(5)	117.8(3)
O(3)–C(6)–C(5)	109.6(3)
O(3)–C(6)–C(2)	111.1(3)
C(5)–C(6)–C(2)	106.5(3)
C(6)–O(3)–Si(1)	120.5(2)
C(3)–N(3)–C(4)	126.4(3)
C(3)–N(3)–H(3)	116.8
C(4)–N(3)–H(3)	116.8
O(2)–C(3)–N(3)	123.1(4)
O(2)–C(3)–C(2)	119.8(4)
N(3)–C(3)–C(2)	117.0(4)
O(1)–C(5)–C(6)	107.0(3)
O(1)–C(5)–C(4)	111.1(3)
C(6)–C(5)–C(4)	111.8(3)
O(1)–C(5)–H(5)	109.0
C(6)–C(5)–H(5)	109.0
C(4)–C(5)–H(5)	109.0
C(1)–N(2)–C(2)	117.8(3)
C(1)–N(1)–H(1A)	120.0
C(1)–N(1)–H(1B)	120.0
H(1A)–N(1)–H(1B)	120.0
N(3)–C(4)–C(5)	114.5(3)
N(2)–C(2)–C(6)	110.4(3)
N(2)–C(2)–C(3)	108.8(3)
C(6)–C(2)–C(3)	110.2(3)
N(2)–C(1)–N(1)	122.6(4)

Table 8 continued

N(2)–C(1)–O(1)	126.9(3)
N(1)–C(1)–O(1)	110.5(4)
C(11)–C(9)–C(10)	108.4(6)
C(11)–C(9)–C(12)	111.1(9)
C(10)–C(9)–C(12)	106.4(6)
C(11)–C(9)–Si(1)	111.1(5)
C(10)–C(9)–Si(1)	110.8(5)
C(12)–C(9)–Si(1)	109.0(6)

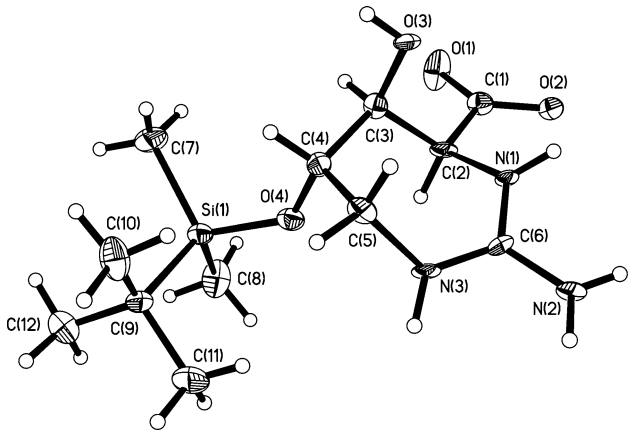

Fig. 1 ORTEP plot of compound **4b**. Thermal ellipsoids are shown at 50% probability

Table 9 Hydrogen bond lengths [Å] and angles [°] for compound **4b**

D–H···A	d (D–H)	d (H···A)	d (D···A)	<(DHA)
O(3)–H(3)···O(2)#1	0.84	1.99	2.805(5)	162.9
N(2A)–H(2AA)···O(2)#2	0.88	2.06	2.914(6)	164.3
N(1A)–H(1A)···O(2)	0.88	2.14	2.987(5)	160.2
N(1)–H(1)···O(1A)	0.88	1.97	2.771(5)	151.0
N(3)–H(3A)···O(2A)#3	0.88	2.07	2.694(5)	126.9
N(2)–H(2A)···O(3A)#4	0.88	2.05	2.863(5)	153.7
O(3B)–H(3B)···O(3C)	0.84	2.16	2.971(5)	163.1
O(3C)–H(3C)···O(2C)#1	0.84	2.01	2.841(6)	171.6
N(1C)–H(1C)···O(1B)	0.88	1.96	2.774(6)	153.3
N(1B)–H(1B)···O(2C)	0.88	2.05	2.877(6)	157.1
N(3B)–H(3BA)···O(1C)#5	0.88	2.05	2.721(6)	132.3
N(3C)–H(3CA)···O(2B)#6	0.88	2.11	2.701(6)	124.1
N(2B)–H(2BA)···O(2C)#5	0.88	2.09	2.941(6)	162.8
N(2C)–H(2CA)···O(3B)#7	0.88	2.21	2.876(6)	132.7
N(3A)–H(3AC)···O(1)#2	0.88	2.05	2.744(6)	134.7

Symmetry transformations used to generate equivalent atoms

#1 $x, y + 1, z$; #2 $-x + 1, y + 1/2, -z + 1$; #3 $-x + 2, y + 1/2, -z + 1$; #4 $-x + 2, y - 1/2, -z + 1$; #5 $-x + 1, y + 1/2, -z$; #6 $-x, y + 1/2, -z$; #7 $-x, y - 1/2, -z$

respective diastereomers **3a** and **4a** (Scheme 3) [3]. Specifically, the oxazole **3b** forms after nucleophilic addition of the alkoxide to the electrophilic carbon in the cyanamide group. Although the two reacting groups are in *trans* orientation, which has been shown to disfavor this attack in the diastereomer **2a**, conformational analysis suggests that the inverted configuration of the bulky TBDMS substituent in **2b** facilitates the ring closure to the oxazole **3b**. Formation of the diazepane **4b** presumably follows the pathway of rearrangement and ring expansion that has been outlined before for the synthesis of **4a** [3]. This reaction likely proceeds via the oxazole intermediate **6** which emerges from the nucleophilic attack of the carbonyl oxygen in **2b** at the cyanamide group. Finally, a third pathway is initiated by migration of the TBDMS group, thereby producing an alkoxide at the 5 position which is well oriented for a transannular attack at the cyanamide (Scheme 3). Facile migration of the silyl substituent has been observed before in the diastereomer **2a**. However, since the configuration of the alkoxide is inverted in **2a**, a comparable addition to the cyanamide cannot be achieved and the ring closure involving the carbonyl oxygen to form the diastereomer of oxazole **6** becomes the dominant alternative. Therefore, we conclude that the novel 2-oxa-4,7-diazabicyclo[3.3.1]non-3-ene heterobicycle in **5** is a unique product emerging from base treatment of **1b**. Despite that the compound **5** was originally obtained as an unexpected side product, the constitution of the heterobicyclic 2-oxa-4,7-diazabicyclo[3.3.1]non-3-ene scaffold renders it an attractive intermediate for the synthesis of RNA-directed ligands. The cup shaped bicyclic system revealed by the crystal structure presents hydrogen bond donors and acceptors on one face of the rigid scaffold while the silyl-protected alcohol on the opposite side allows for further derivatization.

Crystal Structure

Compound **4b** crystallized in the monoclinic $P2_1$ space group with four molecules in the unit cell. An ORTEP drawing of one of the molecules with atom numbering scheme is shown in Fig. 1. The seven-membered ring has a twisted-chair conformation. The twist is evidenced by the torsion angle C(2)–N(1)–C(6)–N(3). This torsion angle ranges from −23.2(3)° to −37.2(3)° with the average value of 29.6° for all four molecules. In the molecule **4b** the ring atoms C(2), C(3), C(5), and N(3) are coplanar to within 0.0186 Å with C(6) and N(1) of 0.729(3) and 0.934(3) Å, respectively, above that plane and C(4) of 0.701(3) Å below (on average). The carboxylic moiety containing C(2), C(1), O(1), and O(2) atoms is rotated along the C(1)–C(2) bond with respect to the main ring. This rotation angle varies from 36.7(5)° to 63.8(5)° with an average value of

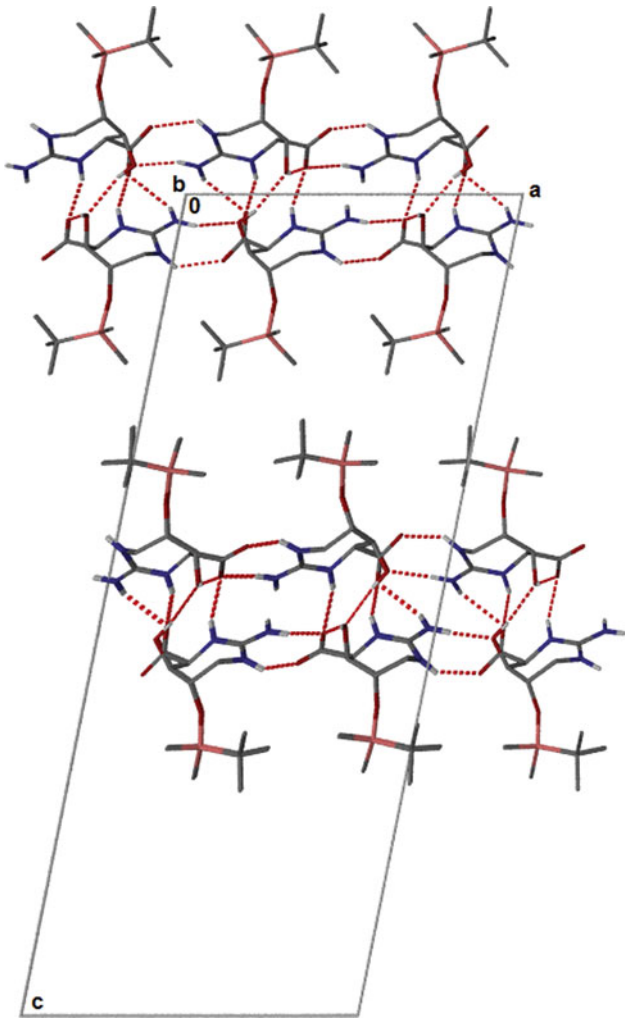

Fig. 2 Intermolecular hydrogen bonding pattern in the crystal of **4b**. Hydrogen bonds are shown as *dashed lines*. The hydrogen atoms involved in the hydrogen bonding network are shown, while the others are omitted for clarity

53.0°. Compound **4b** crystallizes in the form of a zwitterion. While negative charge is located at the O(1)–O(2)–C(1) carboxylic end of the molecule, positive charge is delocalized over N(1)–N(2)–N(3)–C(6) atoms which lie in a plane to within 0.0036 Å (on average). While all C–N bonds in the **4b** molecule posses partial double-bond character [7], C(6)–N(3) bond is consistently the shortest one in all four molecules. It is shorter than any other C(6)–N(1) or C(6)–N(2) bond by 0.017 Å on average. We attribute this to the electron-withdrawing effect of the carboxylic group which exerts stronger influence on the near C–N bonds. This is also supported by the observed C(2)–N(1) and C(5)–N(3) bond lengths. The former one being closer to the carboxyl group is longer on average by 0.004 Å. The OTBDMS and hydroxyl groups in **4b** are in the axial positions on this seven-membered ring. Due to weak intramolecular N(1)–H(1)···O(1) [O(1)···H(1) = 2.313 Å] hydrogen bonding, the carboxylic group is almost coplanar with C(2)–N(1)–H(1) fragment with O(2)–C(1)–C(2)–N(1) torsion angle ranging from 0.4(5)° to 14.1(5)° with an average value of 9.1°. The crystal packing of **4b** is achieved through a complex network of hydrogen bonds occurring between neighboring molecules (Table 9). Four independent molecules of **4b** form two distinct pairs through hydrogen bonding forces. In every pair identical molecules propagate along the *b*-axis. While one of the molecules in each pair uses carboxyl-hydroxyl hydrogen bond interaction for this [H(3)···O(2) = 2.805(5) and 2.841(6) Å], another one is placed in a similar face-to-back fashion through hydrogen bonding interaction with the first molecule in the pair. Molecules of each pair alternate along the *a*-axis. Pairs are separated by a hydrophobic region occupied by the bulky OTBDMS groups. These hydrogen bonding interactions lead to the formation of the complex pattern as shown in Fig. 2.

Compound **5** crystallized in the monoclinic $P2_1$ space group with three molecules in the unit cell. An ORTEP drawing of one of the molecules with atom numbering scheme is shown in Fig. 3. In two of the molecules the OTBDMS group is disordered. While both parts of one such molecule could be modeled as a 0.68/0.32 disorder, disorder in another molecule is more severe. One part of the molecule could be modeled in this 0.66/0.34 disorder and successfully located in the electron density map. However, another part of this molecule could not be reliably located and only silicon and one carbon atom could be

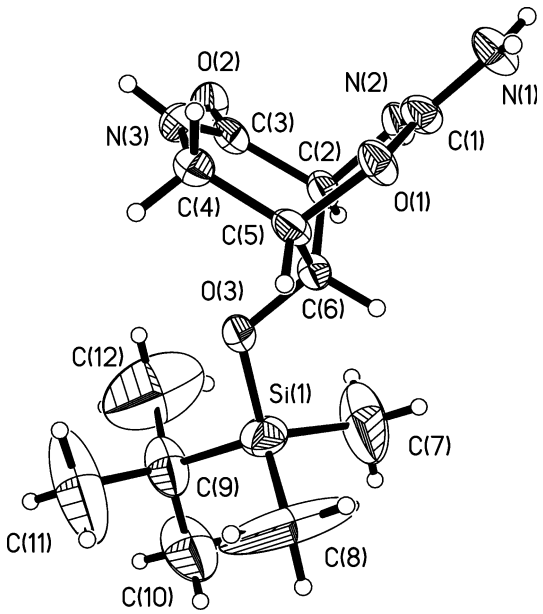

Fig. 3 ORTEP plot of compound **5**. Thermal ellipsoids are shown at 50% probability

placed. The planes of this bicyclic compound, defined by C(1), N(2), C(2), C(5), and O(1) for the first plane and by C(2), C(3), C(4), N(3), and C(5) for the second plane are nearly flat, with 0.0213 and 0.0441 Å average deviation for the first and second plane, respectively. The angle between these planes is 72.9(5)°. The angles between these two planes and the C(2)–C(5)–C(6) plane are almost identical, being 54.0(5)° and 53.2(5)°, respectively. Each of the three molecules of compound **5** forms hydrogen bonds with three neighboring molecules (Table 10). Thus, molecule 1 forms two hydrogen bonds with another molecule 1 along the *c*-axis. Each of the molecules 1 in this pseudo-dimeric unit also forms two hydrogen bonds with molecule 2 along the *c*-axis. Molecule 2 also forms two hydrogen bonds with molecule 3 along the *a*-axis. Molecule 3 forms dimeric chains along the *b*-axis in a fashion similar to the molecule 1. The pseudo-dimer is connected to another molecule 2 via two hydrogen bonds along the *a*-axis. The molecule 2 is in turn connected to another pseudo-dimeric unit of molecules 1 along the *b*-axis. This whole structural motif propagates along the *b*-axis via interactions of molecule 1–molecule 1 (two hydrogen bonds), molecule 2–molecule 2 (one hydrogen bond), and molecule 3–molecule 3 (two hydrogen bonds). Altogether, these complex hydrogen bonding interactions result in the formation of a stair-step motif shown on Fig. 4.

Table 10 Hydrogen bond lengths [Å] and angles [°] for compound **5**

D–H···A	d(D–H)	d(H···A)	d(D···A)	<(DHA)
N(3)–H(3)···O(102)	0.88	2.06	2.921(4)	165.8
N(103)–H(10)···O(2)	0.88	1.99	2.859(4)	168.6
N(1)–H(1A)···O(1)#1	0.88	2.25	3.120(4)	168.1
N(1)–H(1B)···N(2)#2	0.88	2.20	2.951(5)	142.7
N(101)–H(10E)···O(202)#3	0.88	2.11	2.966(5)	163.9
N(101)–H(10F)···O(102)#4	0.88	1.98	2.855(5)	174.6
N(203)–H(20A)···N(102)#5	0.88	2.08	2.858(5)	146.9
N(201)–H(20B)···O(201)#6	0.88	2.16	2.984(5)	156.2
N(201)–H(20C)···N(202)#7	0.88	2.02	2.893(5)	170.8

Symmetry transformations used to generate equivalent atoms

#1 $-x, y + 1/2, -z + 1$; #2 $-x, y - 1/2, -z + 1$; #3 $x - 1, y, z$; #4 $x, y + 1, z$; #5 $x + 1, y, z$; #6 $-x + 1, y + 1/2, -z$; #7 $-x + 1, y - 1/2, -z$

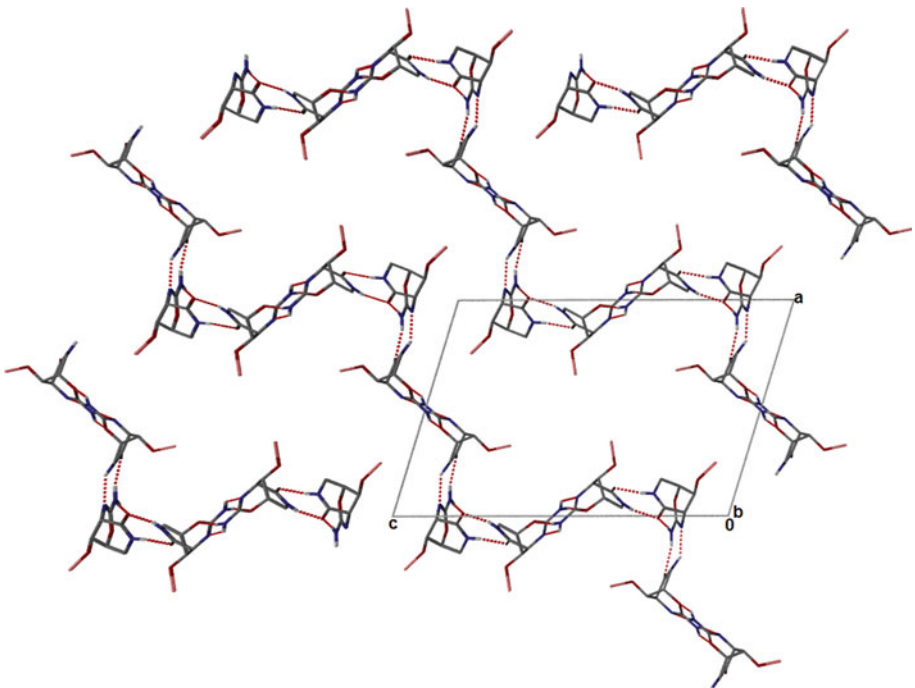

Fig. 4 Intermolecular hydrogen bonding pattern in the crystal of **5**. Hydrogen bonds are shown as *dashed lines*. The hydrogen atoms involved in the hydrogen bonding network are shown, while the others are omitted for clarity

Supplementary Material

CCDC 809138 and 809139 contain the supplementary crystallographic data for this paper. These data can be obtained free of charge by e-mailing data_request@ccdc.cam.ac.uk, or by contacting The Cambridge Crystallographic Data Centre, 12 Union Road, Cambridge CB2 1EZ, UK, Fax: +44(0)1223-336033.

Acknowledgments This study was supported in part by the National Institutes of Health, Grant No. AI72012 and CA132753. Support of the NMR facility by the National Science Foundation is acknowledged (CRIF grant CHE-0741968).

References

1. Poehlsgaard J, Douthwaite S (2005) Nat Rev Microbiol 3:870
2. Thomas JR, Hergenrother PJ (2008) Chem Rev 108:1171
3. Dutta S, Higginson CJ, Ho BT, Rynearson KD, Dibrov SM, Hermann T (2010) Org Lett 12:360
4. Bruker SAINT (2005) Bruker AXS Inc., Madison
5. SADABS: v.2.01 (2001) An empirical absorption correction program, Bruker AXS, Madison
6. Sheldrick GM (1997) SHELX-97, program for crystal structure refinement. University of Gottingen, Germany
7. Uppsala Software Factory—typical bond lengths (1997) http://hhmi.swmed.edu/Manuals/gerard/typical_bonds.html